

The identification of the cosmic-ray light nuclei with the GAPS experiment

Riccardo Munini^{a,b,*} and Alex Lenni^b for the GAPS collaboration

^a*INFN, Sezione di Trieste, I-34149 Trieste, Italy*

^b*IFPU, I-34014 Trieste, Italy*

E-mail: riccardo.munini@ts.infn.it, alex.lenni@sissa.it

GAPS (General AntiParticle Spectrometer) is a balloon-borne large-acceptance experiment designed to detect low-energy (< 0.25 GeV/n) cosmic-ray antinuclei during three ~ 35 -day Antarctic flights, the first of these planned for the 2024-2025 austral summer. The GAPS experiment, currently in preparation for the first flight, consists of a tracker equipped with large-area lithium-drifted silicon detectors and surrounded by a large-acceptance time-of-flight system made of plastic scintillators. This design has been optimized to perform a novel antiparticle identification technique based on an antinucleus capture and the subsequent exotic atom formation and decay, allowing more active target material and a larger geometrical acceptance since no magnet is required. Although detecting the cosmic-ray antinuclei as an indirect dark-matter signature is the primary goal of GAPS, many low-energy cosmic-ray nuclei will also be recorded. Nuclei do not form exotic atoms in the GAPS detectors, and their detection is based on the measurements of the ionization energy depositions, evaluation of the kinetic energy, and the stopping depth relative to the measured velocity. An algorithm was developed to fit the slow-down of particles and antiparticles tracked inside GAPS. The quantities fitted by this algorithm, together with the measured velocity and energy deposition information, allow the identification of protons, deuterons, and helium nuclei and the measurement of their spectra in a low-energy range (< 0.25 GeV/n). The results of this analysis, based on detailed Monte Carlo simulation studies, will be presented in this contribution.

38th International Cosmic Ray Conference (ICRC2023)
26 July - 3 August, 2023
Nagoya, Japan



*Speaker

1. The GAPS experiment

GAPS (General AntiParticle Spectrometer) is a balloon-borne experiment designed to measure low-energy (< 0.25 GeV/ n) cosmic-ray antinuclei, especially antiproton (\bar{p}) and antideuteron (\bar{d}), during a series of three long-duration flights at an altitude of ~ 37 km (~ 7 g cm $^{-2}$ of overhead atmosphere) in Antarctica.

The GAPS experiment includes a multiple-layer tracker equipped with large-area lithium-drifted silicon (Si(Li)) detectors, surrounded by a Time-of-Flight (TOF) system of thin plastic scintillators (see Figure 1). This design has been optimized to perform a novel antiparticle-identification technique based on antinucleus capture and the subsequent exotic atom formation and decay [1] through a series of atomic transitions emitting characteristic X-rays. Finally, the annihilation of the antinucleus with the atomic nucleus produces a nuclear star of several secondary particles, mainly pions and protons, originated from a common vertex. The instrumental design allows a larger geometrical acceptance since no magnet is required. The geometrical acceptance of the order of ~ 10 m 2 sr in the energy range [0.05; 0.25] GeV/ n will enable GAPS to collect large statistics to improve the sensitivities of antiprotons and lightest antinuclei. For more technical and scientific details on the GAPS experiment see [2–7]

The GAPS experiment is scheduled for its first long balloon campaign confirmed for the 2024-2025 Austral summer from the McMurdo station in Antarctica. The polar location is ideal for studies of low-energy cosmic rays because of the very low geomagnetic cut-off.

2. Light-nuclei with GAPS

Although the GAPS experiment is specifically designed for the detection of cosmic-ray antinuclei, the measurement of low-energy cosmic-ray nuclei is possible and well-motivated for several reasons.

- The study of nucleus events with non-interacting single tracks allows to calibrate the instrument and to gain insight into the systematic uncertainties.
- A high statistics test of the identification capabilities with protons and deuterons is preparatory to the \bar{p}/\bar{d} analysis. Additionally, the \bar{p}/\bar{d} identifications will benefit from the information of the annihilation (number of secondaries, X-rays, etc...), which will result in a higher rejection power.
- Nuclei measurements will improve the understanding of the propagation of cosmic-ray light nuclei, especially in the Heliosphere which heavily affects the propagation at low energies. Thanks to the foreseen three flights, the nuclei fluxes will be measured during different conditions of solar activity, allowing to test and calibrate cosmic ray solar modulation models.
- Moreover, models for secondary production in the atmosphere will be tested with a precision of a few percents.

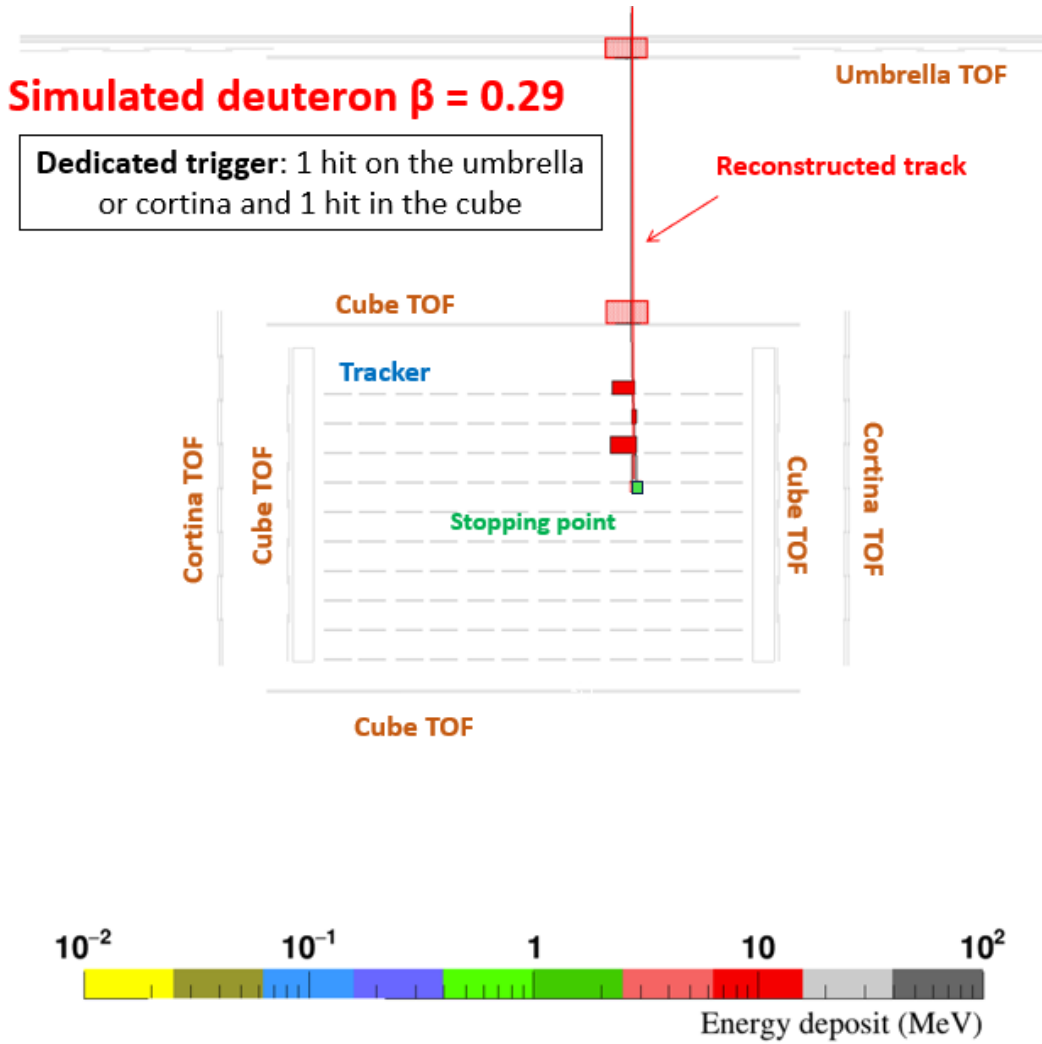


Figure 1: Simulated deuteron with a kinetic energy of 90 MeV/n displayed on the XZ view. The event was selected with the minimum bias trigger requiring one energy deposit in the umbrella ToF and one energy deposit in the upper cube ToF. The black line represents the Monte Carlo trajectory while the red line represented the reconstructed trajectory based on the hit associated with the track.

3. Light-nuclei identification

The identification performance of light nuclei were studied with simulated samples of protons, deuterons, and helium nuclei. These data were generated by a GEANT4-based simulation software developed to reproduce accurately the GAPS apparatus and the radiation-matter interactions inside it. A custom algorithm [8], developed to reconstruct the topology of the annihilation stars generated by the antinuclei stopping inside the GAPS experiment, was used in this case to reconstruct the primary tracks of non-interacting nucleus. In contrast to antinuclei, the stopping nuclei inside the GAPS instrument do not form exotic atoms in the target material.

A minimum bias trigger was required to select non-interacting nuclei. The trigger requires a coincidence between one hit in the Umbrella or Cortina ToF and one hit in the Cube ToF. This

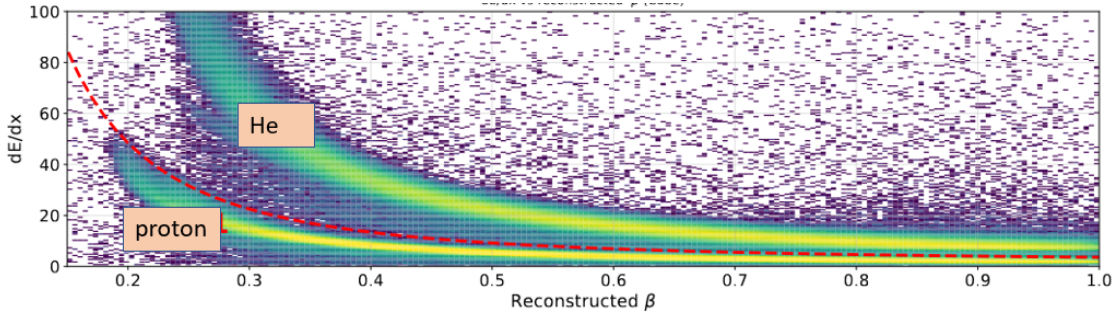


Figure 2: The dE/dx deposited in the cube ToF for simulated helium nuclei and protons. The red dotted line represents a selection cut that provides a proton contamination less than 1% over the whole velocity range.

trigger, in flight, would result in rates greater than 50 kHz. For this reason, the minimum bias trigger will be prescaled with a trigger specifically designed for annihilating events which will result in a rate of less than 100 Hz.

In addition, only events crossing the Umbrella and top Cube downward were selected to reduce the component of secondary produced in the atmosphere, which is more relevant for very inclined events. A dedicated analysis of spectra measured at different angles will be performed. Figure 1 shows an example of a simulated deuteron with a kinetic energy of 90 MeV/ n stopping in the tracker. The solid black line represents the simulated trajectory and the colored rectangular boxes represent the digitized energy deposits (the color code for the energy is represented by the bottom palette). The red line represents the reconstructed trajectory obtained with the hits associated with the primary tracks which are the red dots. With a sample of events that survived these pre-selections, the proton, deuteron, and helium separation was performed.

3.1 Helium nuclei selection

Helium nuclei selection is performed by means of the specific energy release which, according to the Bethe-Block formula, for particles with electric charge $Z = 2$ is four times higher than $Z = 1$ particles. Figure 2 shows the dE/dX measured in the ToF Cube as a function of the reconstructed β ¹. The dotted red line represents the helium nuclei selection which results in a proton contamination of less than 1%. This cut allows to select helium nuclei with a negligible proton contamination over the whole velocity range.

3.2 Deuteron selection

The isotopic separation between proton and deuteron requires additional selections since both are $Z = 1$. Relativistic hydrogen isotopes release the same dE/dX values as a function of β . The selection of protons and deuterons is performed by exploiting their different kinetic energies and consequently the different ranges inside the tracker.

In order to estimate the kinetic energy and other quantities, a fit of the slow-down profile of the particles is performed. The fit is done using the energy deposits of the primary track. At least three hit are necessary in order to perform the fit, thus only events with at least one hit in the tracker are considered. The kinetic energy, the mass of the particle, and the range expressed in cm^2/g are

¹ β is defined as the ratio between the particle velocity v and the speed of light c , $\beta=v/c$

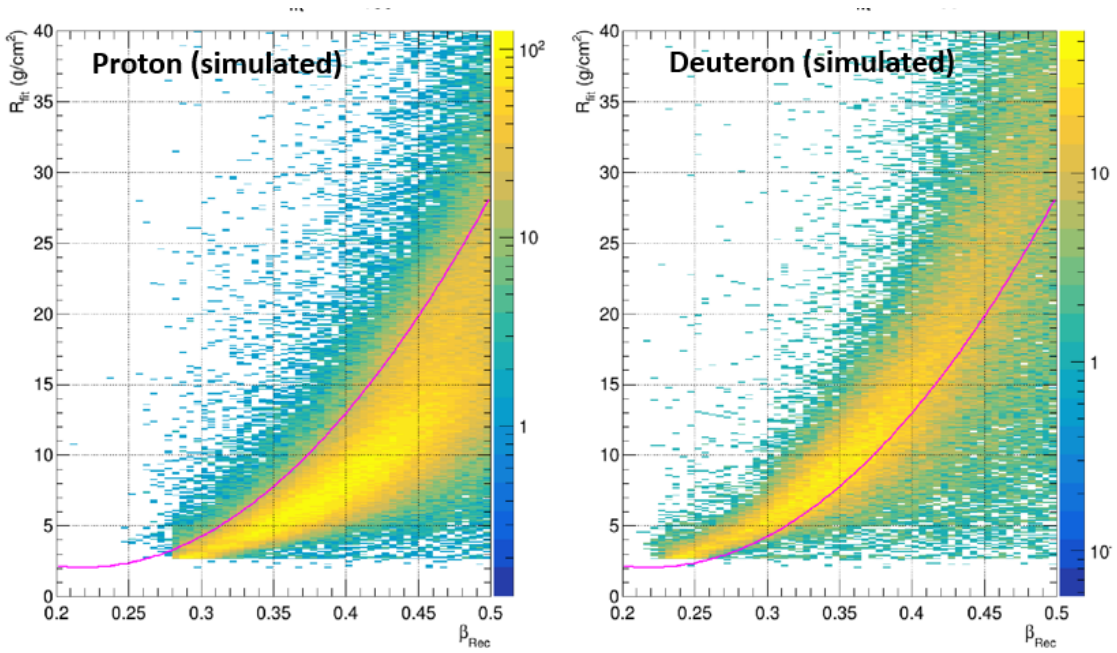


Figure 3: Range evaluated from the slow down fit as a function of the reconstructed β .

obtained. Combining cuts on these variables, the deuteron selection is performed. As an example, Figure 3 shows the estimated range as a function of β for simulated proton (left panel) and deuteron (right panel). It can be noticed that for the same β , deuterons are more penetrating and traverse more material. The red line represents the deuteron selection cut. Combining several of these selections is possible to obtain a clean deuteron sample.

Finally, the most relevant quantities for the deuteron identification turned out to be the dE/dX release in the Umbrella, the estimated mass of the particle, the estimated kinetic energy and the estimated range. In order to obtain the best performances, all these quantities were used as input of a Recurrent Neural Network (RNN) known as Long-Short Term Memory (LSTM) [9] trained on the samples of simulated protons and deuterons.

4. Performance

The performance was studied in terms of acceptance and rejection power. The top panel of Figure 4 shows the deuteron acceptance for the minimum bias trigger configuration (green points) as a function of the simulated kinetic energy per nucleon at the top of the instrument (TOI). The acceptance is almost constant above 30 MeV/n and decreases below this value due to events that stop in the Umbrella ToF. In the same figure, the red points represent the deuteron acceptance after the selection cuts. It has to be noticed that selecting only events crossing the Umbrella and the top Cube decrease the acceptance by more than a factor of 2 since this requirements reduce significantly the angular aperture of the instrument. The blue point represents the contaminating protons.

The rejection power, defined as ratio of the deuteron over proton acceptance, is represented in the lower panel of Figure 4. The light blue, orange and green arrows in the picture are benchmark values corresponding to a 1%, 3% and 6% of residual proton contamination in the deuteron sample

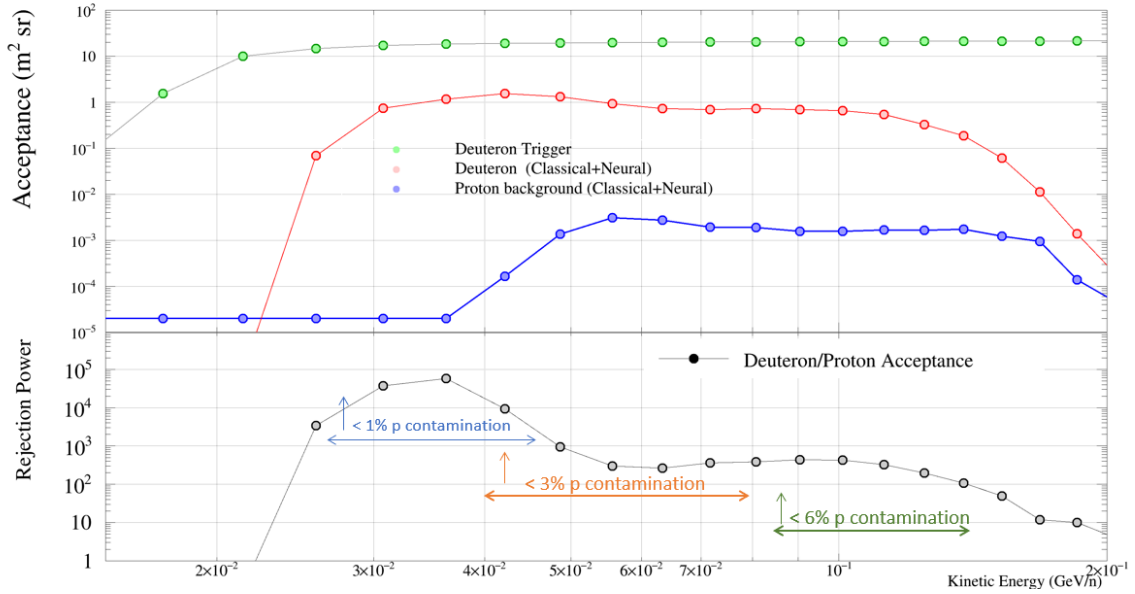


Figure 4: Top panel: Deuteron acceptance after the minimum bias trigger (green points) and after the selection cuts and neural network analysis (red points) as a function of the simulated TOI kinetic energy (see text for TOA conversion). The acceptance corresponding to the contaminating protons is represented by the blue dots. Bottom panel: Ratio of the deuteron over proton acceptances (gray points) and proton contamination value according to the cosmic-ray proton and deuteron fluxes near Earth.

considering typical value of cosmic-ray fluxes near Earth. With this preliminary analysis, it is observed that GAPS allows to measure deuterons with a low proton contamination from ~ 30 to ~ 100 MeV/ n . These energy intervals correspond to ~ 80 and ~ 130 MeV/ n when expressed in terms of top of the atmosphere (TOA) energy values. The conversion was done running the PLANETOCOSMIC² simulation tool and accounting for the atmospheric attenuation for cosmic ray detected at ~ 37 km.

Figure 5 shows the acceptance and rejection power for helium nuclei. In this case the residual proton contamination is well below 1% over the whole kinetic energy range. It has been estimated that according to the β resolution, for helium nuclei (and protons) a measurements of the fluxes up to 1 GeV/ n (considering bins of 3 times the resolution in β) is feasible.

5. Conclusions and perspectives

This preliminary work demonstrates the capabilities of light nuclei detection and identification with GAPS, an instrument specifically designed for antinucleus detection. With the estimated acceptance and the expected trigger configuration, the fluxes will be measured with a statistical precision of about a percent for deuterons and on the order of per mill for helium nuclei and protons. These measurements will allow to improve the understanding of the cosmic ray light nuclei propagation, especially in the Heliosphere which heavily affects cosmic rays at these energies.

²<http://cosray.unibe.ch/~laurent/planetocosmics/>

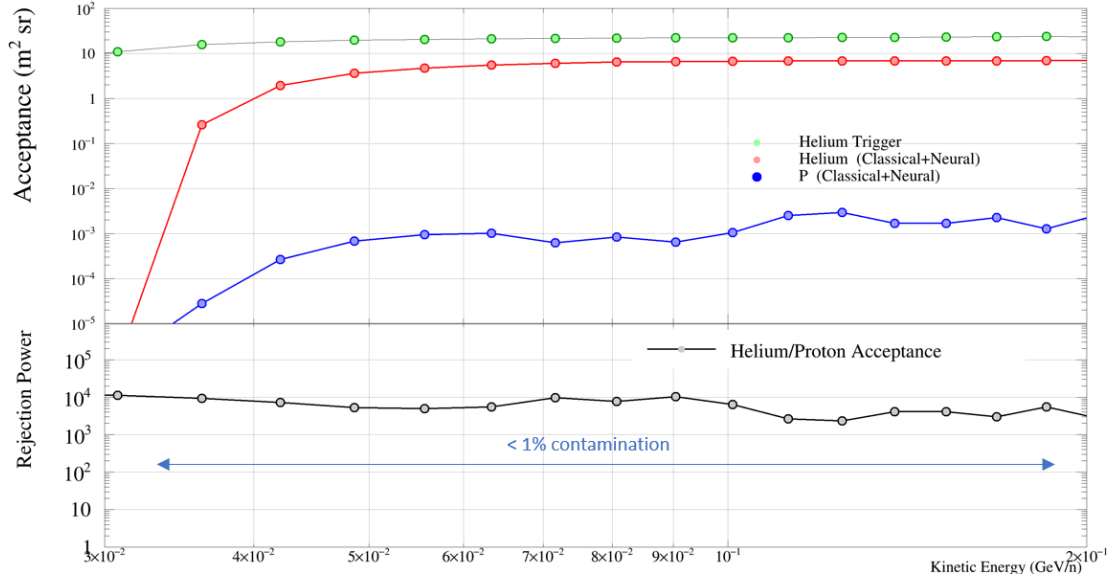


Figure 5: Top panel: Helium nuclei acceptance after the minimum bias trigger (green points) and after the selection cuts and neural network analysis (red points) as a function of the simulated TOI kinetic energy. The acceptance corresponding to the contaminating protons is represented by the blue dots. Bottom panel: Ratio of the helium over proton acceptances (gray points) and proton contamination value according to the proton and deuteron flux near Earth.

Furthermore, models for secondary production in the atmosphere will be tested. The next steps of this work will be:

- Improving the proton rejection power to reach negligible contamination for deuterons at least up to 200 MeV/n.
- Estimate secondary protons, deuterons, and helium nuclei produced in the residual atmosphere. This will help to validate and improve models for secondary production allowing to separate and study the Galactic component.

References

- [1] T. Aramaki et al., *Astroparticle Physics* 74, 6 2016
- [2] K. Mori et al., deexcitation of exotic atoms,” *ApJ* vol. 566, 2002
- [3] C.J. Hailey, *New J Phys.*, vol. 11, 2009
- [4] T. Aramaki et al., *Astropart. Phys.*, vol. 74, 6–13, 2016
- [5] T. Aramaki et al., *Astropart. Phys.*, vol. 59, 12–17, 2014
- [6] N. Saffold et al., *Astropart. Phys.*, vol. 130, 102580, 2021

- [7] F. Rogers et al., *Astropart. Phys.*, vol. 145, 2023
- [8] R. Munini et al., *Astroparticle Physics* 133, 102640, 2021
- [9] S. Hochreiter and J. Schmidhuber, *Neural computation*. 9. 1735-80, 1997

Full Authors List: GAPS

T. Aramaki¹, M. Boezio^{2,3}, S. E. Boggs⁴, V. Bonvicini², G. Bridges⁵, D. Campana⁶, W. W. Craig⁷, P. von Doetinchem⁸, E. Everson⁹, L. Fabris¹⁰, S. Feldman⁹, H. Fuke¹¹, F. Gahbauer⁵, C. Gerrity⁸, L. Ghislotti^{15,16}, C. J. Hailey⁵, T. Hayashi⁵, A. Kawachi¹², M. Kozai¹³, P. Lazzaroni^{15,16}, M. Law⁵, A. Lenzi³, A. Lowell⁷, M. Manghisoni^{15,16}, N. Marcelli¹⁸, K. Mizukoshi²⁷, E. Mocchiutti^{2,3}, B. Mochizuki⁷, S. A. I. Mognet¹⁹, K. Munakata²⁰, R. Munini^{2,3}, S. Okazaki²⁷, J. Olson²², R. A. Ong⁹, G. Osteria⁶, K. Perez⁵, F. Peretto⁶, S. Quinn⁹, V. Re^{15,16}, E. Riceputi^{15,16}, B. Roach²³, F. Rogers⁷, J. L. Ryan⁹, N. Saffold⁵, V. Scotti^{6,24}, Y. Shimizu²⁵, K. Shutt⁷, R. Sparvoli^{17,18}, A. Stoessl⁸, A. Tiberio^{26,29}, E. Vannuccini²⁶, M. Xiao²³, M. Yamatani¹¹, K. Yee²³, T. Yoshida¹¹, G. Zampa², J. Zeng¹, and J. Zweerink⁹

¹Northeastern University, 360 Huntington Avenue, Boston, MA 02115, USA ²INFN, Sezione di Trieste, Padriciano 99, I-34149 Trieste, Italy ³IFPU, Via Beirut 2, I-34014 Trieste, Italy ⁴University of California, San Diego, 9500 Gilman Dr., La Jolla, CA 90037, USA ⁵Columbia University, 550 West 120th St., New York, NY 10027, USA ⁶INFN, Sezione di Napoli, Strada Comunale Cinthia, I-80126 Naples, Italy ⁷Space Sciences Laboratory, University of California, Berkeley, 7 Gauss Way, Berkeley, CA 94720, USA ⁸University of Hawai'i at Mānoa, 2505 Correa Road, Honolulu, Hawaii 96822, USA ⁹University of California, Los Angeles, 475 Portola Plaza, Los Angeles, CA 90095, USA ¹⁰Oak Ridge National Laboratory, 1 Bethel Valley Rd., Oak Ridge, TN 37831, USA ¹¹Institute of Space and Astronautical Science, Japan Aerospace Exploration Agency (ISAS/JAXA), Sagami-hara, Kanagawa 252-5210, Japan ¹²Tokai University, Hiratsuka, Kanagawa 259-1292, Japan ¹³Polar Environment Data Science Center, Joint Support-Center for Data Science Research, Research Organization of Information and Systems, (PEDSC, ROIS-DS), Tachikawa 190-0014, Japan ¹⁵Università di Bergamo, Viale Marconi 5, I-24044 Dalmine (BG), Italy ¹⁶INFN, Sezione di Pavia, Via Agostino Bassi 6, I-27100 Pavia, Italy ¹⁷INFN, Sezione di Roma "Tor Vergata", Piazzale Aldo Moro 2, I-00133 Rome, Italy ¹⁸Università di Roma "Tor Vergata", Via della Ricerca Scientifica, I-00133 Rome, Italy ¹⁹Pennsylvania State University, 201 Old Main, University Park, PA 16802 USA ²⁰Shinshu University, Matsumoto, Nagano 390-8621, Japan ²²Heliospace Corporation, 2448 6th St., Berkeley, CA 94710, USA ²³Massachusetts Institute of Technology, 77 Massachusetts Ave., Cambridge, MA 02139, USA ²⁴Università di Napoli "Federico II", Corso Umberto I 40, I-80138 Naples, Italy ²⁵Kanagawa University, Yokohama, Kanagawa 221-8686, Japan ²⁶INFN, Sezione di Firenze, via Sansone 1, I-50019 Sesto Fiorentino, Florence, Italy ²⁷Research and Development Directorate, Japan Aerospace Exploration Agency (JAXA), 2-1-1 Sengen, Tsukuba 305-8505, Japan ²⁸Research and Development Directorate, Japan Aerospace Exploration Agency, Sagami-hara, Kanagawa 252-5210, Japan ²⁹Università degli studi di Firenze, via Sansone 1, I-50019 Sesto Fiorentino, Florence, Italy